

Compact Long-Period Fiber Gratings Based on Periodic Microchannels

Jing-Chun Guo, Yong-Sen Yu, Yang Xue, Chao Chen, Rui Yang,
Chuang Wang, Qi-Dai Chen, and Hong-Bo Sun, *Member, IEEE*

Abstract—A novel formation method of long-period fiber gratings (LPGs) based on periodic microchannels, which are fabricated by femtosecond laser micromachining and selective chemical etching in conventional single-mode fibers, is proposed and experimentally demonstrated. This kind of grating may be as short as only 3 mm and exhibits low-temperature sensitivity of 9.95 pm/°C from 30 °C to 120 °C. The strain sensitivities of the resonant wavelength and peak loss are -2.4 nm/mε and -3.5 dB/mε, respectively. High refractive-index (RI) sensitivity with one order of magnitude larger than that of the conventional LPGs near RI = 1.33 is achieved in general single-mode fibers.

Index Terms—Femtosecond laser, fiber sensor, long-period fiber gratings (LPGs), microchannels.

I. INTRODUCTION

IN RECENT years, the femtosecond (fs) laser micromachining technology has been widely applied in transparent materials because of the high spatial resolution and three-dimensional (3-D) controllable micromachining characteristics [1]–[3]. For this reason, long period fiber gratings (LPGs) fabrication was demonstrated by direct fs laser writing to achieve high temperature sensing [4], [5]. As an ideal refractive index (RI) sensing element, the RI sensitivity reaches the maximum value when the surrounding RI approaches to the effective index of the cladding mode for conventional LPGs [5], [6], however, a much lower sensitivity of only ten's of nm/RI unit (RIU) is obtained near RI = 1.33. D. N. Wang et al. reported a type of microhole-structured LPGs fabricated by fs laser direct ablation in all-solid photonic bandgap fibers [7] and photonic crystal fibers (PCFs) [8], [9]. The microhole-structured LPGs were made by drilling holes from the surface to the fiber core in just one side of the fibers, they have normal period (~ 500 μm) but exhibit compact size and much higher RI sensitivity [7]. The microhole-structured LPGs in two types of PCFs both have large polarization dependent loss (PDL) that induced by the just one side asymmetry structure modulation [7], [8]. The etching rate of the fs-laser-modified silica region is found to be higher than the unmodified one in hydrofluoric acid (HF) solution with volume concentration of

5% [10], a general approach includes fs laser spatial patterning followed with a chemical etching process is found to achieve 3-D microchannels structures inside a volume of silica glass. After that, the combination of the fs laser micromachining and chemical etching technique has been widely used to fabricate lots of microstructures such as microchannels inside bulk glass [10]–[12], microchannels [13], micro-slot [14], and micro-hole array [15] in conventional single-mode fibers (SMFs). These microstructures have been used as lab-on-a-chip device to detect single red blood cell [12] and RI sensors [13]–[15]. In this letter, we report a novel type of LPGs based on periodic microchannels (PMC), which are fabricated by fs laser direct writing and subsequent HF etching in SMFs. Strong RI modulation in both the fiber core and cladding is obtained to induce the coupling of the core mode to the cladding mode. Besides a good linear relationship between the PMC LPG and the axial strain, the PMC LPG has low temperature sensitivity and high RI sensitivity of one order of magnitude larger than that of the conventional LPGs near RI = 1.33.

II. EXPERIMENTS

Direct writing of the periodic straight-line laser-modified structure in standard SMFs (Corning SMF-28) with infrared fs laser pulses was conducted with a Ti:sapphire regenerative amplifier laser system (Spectra Physics) operating at 800 nm. The pulse duration and the repetition rate were 100 fs and 1 kHz, respectively. The laser beam was focused via an oil-immersed 60 × Olympus objective (N.A., 1.42). The diameter of the focal point was estimated to be 0.68 μm. The energy of laser beam was adjusted by a neutral density filter. The fiber was mounted on a computer-controlled three-axis translation stage with a motion spatial resolution of 20 nm. With the help of CCD camera mounted behind the microscope, the fiber core was displayed clearly on computer screen, so we can make sure that the focal point passed through the optical fiber core in the fabrication process. The transmission spectral change was monitored during the fabrication process by a broadband light source (Superk Compact, NKT Photonics) and an optical spectrum analyzer (AQ6370B, Yokogawa). The fiber moved perpendicular to the direction of the laser incident in the fabrication process to realize the straight-line laser-modified structure transversely through the fiber core as shown in Fig. 1(a). Due to the curved surface of the fiber and large RI difference between the air and cladding, the incident laser beam can be defocused to make the focal point distorted. So the fiber and the objective were totally

Manuscript received September 27, 2012; accepted November 7, 2012. Date of publication November 15, 2012; date of current version January 8, 2013. This work was supported in part by the National Natural Science Foundation of China under Grant 90923037 and Grant 91123027.

The authors are with the State Key Laboratory on Integrated Optoelectronics, College of Electronic Science and Engineering, Jilin University, Changchun 130012, China (e-mail: yuys@jlu.edu.cn; hbsun@jlu.edu.cn).

Color versions of one or more of the figures in this letter are available online at <http://ieeexplore.ieee.org>.

Digital Object Identifier 10.1109/LPT.2012.2227701

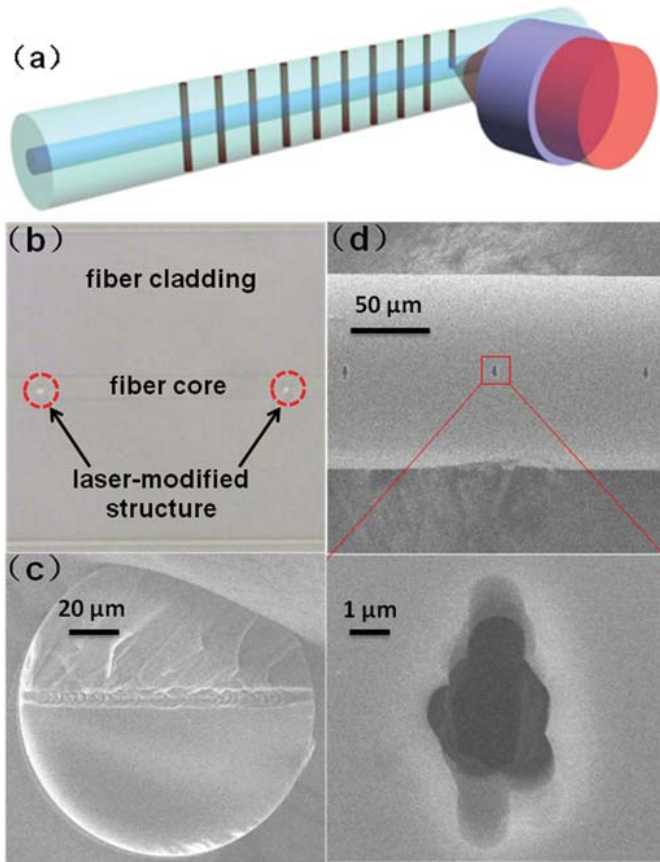


Fig. 1. (a) Schematic diagram of the periodic straight-line laser-modified structure by fs laser direct writing. (b) Microscope image of the periodic straight-line laser-modified waveguides intersecting the fiber core with a period of $100\ \mu\text{m}$ before HF etching. (c) Cross-sectional view. (d) Side-viewed SEM images of the PMC structure with a period of $100\ \mu\text{m}$.

immersed into index-matching oil with RI of 1.5 to alleviate the distortions in the fabrication process. In fact, the focal position almost has no change with the beam position along the fiber section in our calculation after immersed into index-matching oil. The fiber moved $140\ \mu\text{m}$ to make sure that the focal point travelled through the entire fiber to achieve the periodic structure. Fig. 1(b) indicates that the straight-line laser-modified waveguides intersect the fiber core.

To obtain the PMC LPFGs, the periodic laser-modified straight-line structured fiber was immersed in a HF aqueous solution with volume concentration of 4% to achieve selective corrosion. The etching thanks to the HF occurs mainly at the focus point of the beam because the laser-modified feature can be etched >200 times than the nonmodified regions [13]. The scanning electron microscopic (SEM) images in Fig. 1(d) show the side view of the PMC structure with a period of $100\ \mu\text{m}$. The cross-sectional SEM image of the PMC LPFGs is shown in Fig. 1(c), indicating that the microchannels intersect the entire optical fiber section. The PMC structure introduces a strong RI modulation in both the fiber core and cladding, leading to the coupling of the core mode to the cladding mode. A typical transmission spectra change in chemical etching process is shown in Fig. 2, the period and the length of the PMC LPFG are $100\ \mu\text{m}$ and 3 mm, respectively. A little loss

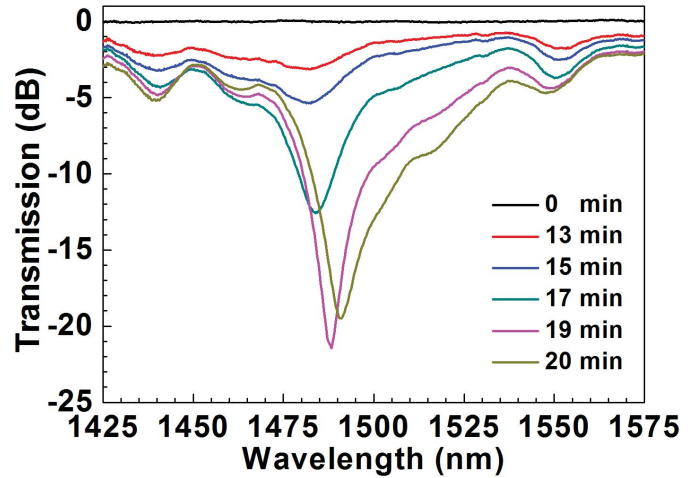


Fig. 2. Evolution of the transmission spectrum of the PMC LPFG in 4% HF etching process.

peak appears after 13 min of chemical etching, indicating that most of the laser-modified region in the cladding has been eroded and the fiber core mode evanescent field is extending into the HF solution. The resonant wavelength has a redshift and the peak loss increases from the 13th min to the 19th min. However, the peak loss begins to decrease in the 20th min due to the over-coupling effect. So the transmission spectrum of the PMC LPFG in the 19th min is what we want. The resonant wavelength and peak loss are both depend on the HF etching time. So we can obtain the desired spectra of the PMC LPFGs by controlling the etching time of 4% HF aqueous solution.

III. SENSING CHARACTERISTICS

After the fabrication process, we studied the sensing characteristics of the PMC LPFG. Although the PMC LPFG had a very short length, it was still sensitive to the curvature. So, when we measured the other parameters, the PMC LPFG must be kept straight to prevent from bend-induced spectral changes. The temperature response was first investigated. The PMC LPFG was mounted on a hot plate with a temperature resolution of $0.1\ ^\circ\text{C}$. The hot plate was heated up from $30\ ^\circ\text{C}$ to $120\ ^\circ\text{C}$ in steps of $5\ ^\circ\text{C}$. It is found that as the temperature increases, the resonant wavelength has a redshift as shown in Fig. 3. The temperature sensitivity is $9.95\ \text{pm}/^\circ\text{C}$ with linearity of 0.995 from a linear fit in the range of $30\ ^\circ\text{C} \sim 120\ ^\circ\text{C}$, which is much smaller than the conventional LPFGs [6]. So these PMC LPFGs are proper for sensing applications to reduce the cross-talk sensitivity from temperature variation.

Although the temperature sensitivity is very low, the thermal effect is still required to be avoided in practical measurements of axial strain and RI. So we measured the axial strain and RI characteristics in a super clean room and the temperature was kept at $22\ ^\circ\text{C}$ all the time. The response to strain is measured by applying axial tension to the PMC LPFGs. It is found that as the axial tension increases, the resonant wavelength of the PMC LPFG has a blueshift and the peak loss increases.

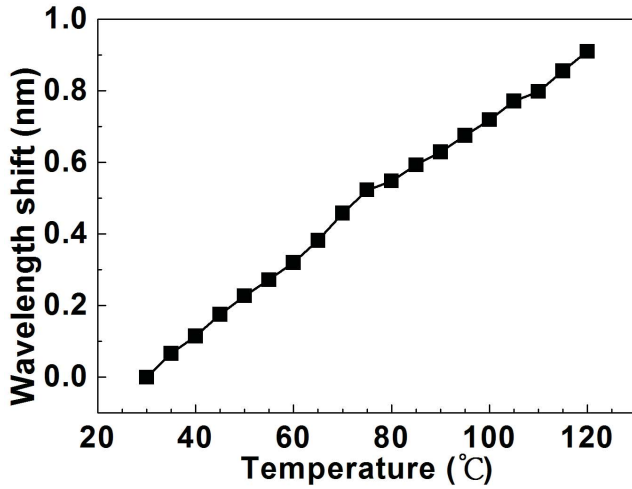


Fig. 3. Shift of the resonant wavelength with different temperatures.

The axial tension is applied from 0 N \sim 1.1 N with an increment of 0.1 N. The cladding in 5% HF has an etching rate of 0.06 $\mu\text{m}/\text{min}$ [13], and the diameter of the microchannel is only about 3 μm , so after 20 min's 4% HF etching, the reduction of the fiber diameter can be neglected. But the axial strength has a large reduction (the PMC LPFG can only bear 2000 $\mu\epsilon$ in our experiment). The material of the rest portion is still silica and the volume of the microchannels is so small that the Young's modulus remains unchanged. So the strain inside the fiber can be calculated by $\epsilon = F/\pi r^2 E$, where F is the axial tension, r is the cladding radius, and E is the silica Young's modulus. The change of the resonant wavelength and peak loss with the applied increasing strain are shown in Fig. 4, both of them have good linear relationships. The average strain sensitivities are $-2.4 \text{ nm}/\text{m}\epsilon$ and $-3.5 \text{ dB}/\text{m}\epsilon$ from a linear fit to the experimental data, respectively, which are of the same magnitude as that of LPFGs as reported in [6].

The RI sensitivity of the PMC LPFG was then measured. The PMC LPFG was placed into a hard plastic slot and kept straight. After the PMC LPFG was fixed, the RI solutions were injected into the plastic tube so that the LPFG was totally immersed. After the spectrum was recorded, the PMC LPFG was then cleaned with ethanol and pure water, and dried by compressed air. The procedure was repeated to measure the other RI solutions (different volume ratio of glycerin and water mixed solutions). The RI of the solution was calibrated by an Abbe refractometer. The resonant wavelength and peak loss in different RI solutions are shown in Fig. 5. The average resonant wavelength RI sensitivities in the RI ranges of 1.333 \sim 1.349 and 1.349 \sim 1.37 are $-692 \text{ nm}/\text{RIU}$ and $-391 \text{ nm}/\text{RIU}$, respectively. The peak loss sensitivities in the RI ranges of 1.333 \sim 1.343 and 1.343 \sim 1.37 are about 1289 dB/RIU and 511 dB/RIU, respectively. Starting from RI of 1.37, the loss peak becomes weaker and weaker and finally disappears. The RI sensitivity of the resonant wavelength is one order of magnitude higher than that of the conventional LPFGs near 1.33 [6]. The RI solutions can fill the PMC structure when the PMC LPFG is immersed, so the RI solutions directly interact with both the core mode and the cladding

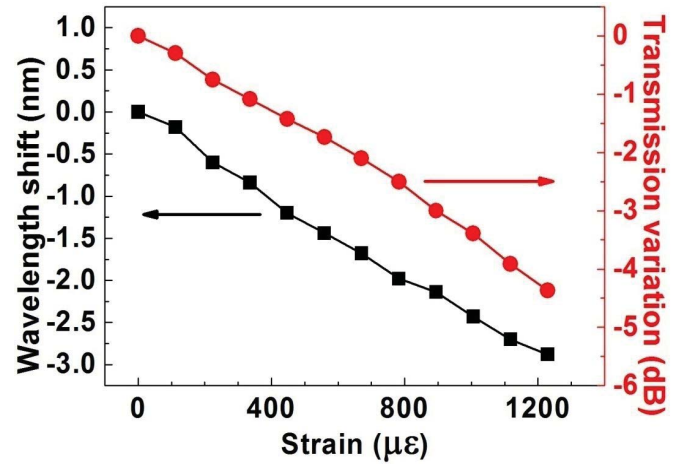


Fig. 4. Shift of the resonant wavelength and peak loss with different axial tension.

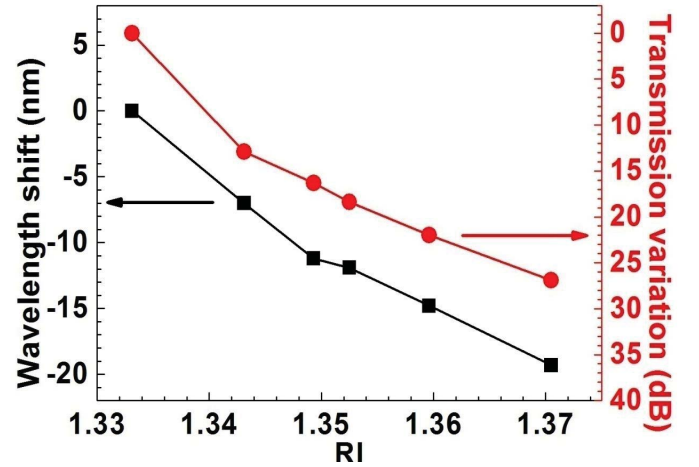


Fig. 5. Shift of the resonant wavelength and peak loss with different RI solutions.

mode. This may be the reason why the PMC LPFG has high RI sensitivities. Furthermore, the RI sensitivity of the peak loss also has one order of magnitude improvement compared with just one microchannel in conventional SMF [13]. Obviously, more microchannels introduce larger interaction area between the light and the ambient matter.

In addition, the polarization response of the PMC LPFGs was checked and we found that the device is insensitive to polarization. Even though we cannot measure the PDL of the PMC LPFGs, but in comparison with the PDL ($< 0.08 \text{ dB}$) of just one microchannel in conventional SMF [13], we deduce the PDL of PMC LPFGs is also insignificant.

IV. DISCUSSION

In general, the phase-matching condition of LPFGs is usually written as:

$$\lambda_{\text{res}} = \left(n_{\text{co}}^{\text{eff}} - n_{\text{cl},m}^{\text{eff}} \right) \Lambda \quad (1)$$

where λ_{res} is the resonant wavelength, Λ is the grating period, and $n_{\text{co}}^{\text{eff}}$ and $n_{\text{cl},m}^{\text{eff}}$ are the effective indices of the guided mode and the m th cladding mode, respectively [6]. In classical

LPPGs, $n_{\text{co}}^{\text{eff}}$ is insensitive to the variation of the external RI. However, $n_{\text{cl,m}}^{\text{eff}}$ is sensitive to the variation of the external RI especially when the external RI is close to $n_{\text{cl,m}}^{\text{eff}}$ due to the disappearance of the cladding mode and the coupling of the guided mode to the radiation modes. So the classical LPPGs have greatest RI sensitivity when the external RI is close to $n_{\text{cl,m}}^{\text{eff}}$. Big difference between the PMC LPPGs and the classical LPPGs is that $n_{\text{co}}^{\text{eff}}$ and $n_{\text{cl,m}}^{\text{eff}}$ are both sensitive to the variation of the external RI in the PMC LPPGs. $n_{\text{cl,m}}^{\text{eff}}$ has a low sensitivity near $\text{RI} = 1.33$, on the contrary, $n_{\text{co}}^{\text{eff}}$ may be most sensitive to the variation of the external RI near 1.33 because the loss peak is the largest in water. As a result, the difference between $n_{\text{co}}^{\text{eff}}$ and $n_{\text{cl,m}}^{\text{eff}}$ is most sensitive to the variation of the external RI when the RI is near 1.33. A small variation of the external RI near 1.33 can induce substantial change to the difference between $n_{\text{co}}^{\text{eff}}$ and $n_{\text{cl,m}}^{\text{eff}}$. This may be the reason why the PMC LPPG has greater RI sensitivity near $\text{RI} = 1.33$.

V. CONCLUSION

In conclusion, we have demonstrated a novel type of PMC LPPGs fabricated by fs laser micromachining and chemical etching technology in conventional SMFs. Strong RI modulation in both the fiber core and cladding is obtained to achieve the coupling between the core mode and the cladding mode. The length and period of the PMC LPPGs are 3 mm and 100 μm , respectively. A low temperature sensitivity of 9.95 $\text{pm}/^\circ\text{C}$ from 30 $^\circ\text{C}$ to 120 $^\circ\text{C}$ is achieved, making these PMC LPPGs suitable candidates for sensing applications to reduce the cross-talk sensitivity from temperature variation. The resonant wavelength and peak loss both have linear response to axial strain with sensitivities of $-2.4 \text{ nm}/\text{m}\epsilon$ and $-3.5 \text{ dB}/\text{m}\epsilon$, respectively. For RI sensing, higher sensitivities of $-692 \text{ nm}/\text{RIU}$ in the RI range of 1.333 \sim 1.349 and 1289 dB/RIU in the RI range of 1.333 \sim 1.343 are achieved due to the direct interaction of the ambient matter with both the core mode and the cladding mode. This type of fiber grating can be used in chemical and physical sensing fields.

REFERENCES

- [1] W. Xiong, *et al.*, "Simultaneous additive and subtractive three-dimensional nanofabrication using integrated two-photon polymerization and multiphoton ablation," *Light, Sci. Appl.*, vol. 1, no. e6, 2012.
- [2] Y. L. Zhang, Q. D. Chen, H. Xia, and H. B. Sun, "Designable 3D nanofabrication by femtosecond laser direct writing," *Nanotoday*, vol. 5, no. 5, pp. 435–448, Dec. 2010.
- [3] Y. L. Sun, *et al.*, "Dynamically tunable protein microlenses," *Angew. Chem. Int. Ed.*, vol. 51, no. 7, pp. 1558–1562, 2012.
- [4] Y. Kondo, K. Nouchi, T. Mitsuyu, M. Watanabe, P. G. Kazansky, and K. Hirao, "Fabrication of long-period fiber gratings by focused irradiation of infrared femtosecond laser pulses," *Opt. Lett.*, vol. 24, no. 5, pp. 646–648, May 1999.
- [5] J. C. Guo, *et al.*, "Compact long-period fiber gratings with resonance at second-order diffraction," *IEEE Photon. Technol. Lett.*, vol. 24, no. 16, pp. 1393–1395, Aug. 15, 2012.
- [6] X. W. Shu, L. Zhang, and I. Bennion, "Sensitivity characteristics of long-period fiber gratings," *J. Lightw. Technol.*, vol. 20, no. 2, pp. 255–266, Feb. 2002.
- [7] M. W. Yang, D. N. Wang, Y. Wang, and C. R. Liao, "Long period fiber grating formed by periodically structured microholes in all-solid photonic bandgap fiber," *Opt. Express*, vol. 18, no. 3, pp. 2183–2189, Feb. 2010.
- [8] S. J. Liu, L. Jin, W. Jin, D. N. Wang, C. R. Liao, and Y. Wang, "Structural long period gratings made by drilling micro-holes in photonic crystal fibers with a femtosecond infrared laser," *Opt. Express*, vol. 18, no. 6, pp. 5496–5503, Mar. 2010.
- [9] S. J. Liu, L. Jin, W. Jin, Y. P. Wang, and D. N. Wang, "Fabrication of long-period gratings by femtosecond laser-induced filling of air-holes in photonic crystal fibers," *IEEE Photon. Technol. Lett.*, vol. 22, no. 22, pp. 1635–1637, Nov. 15, 2010.
- [10] A. Marcinkevičius, *et al.*, "Femtosecond laser-assisted three-dimensional microfabrication in silica," *Opt. Lett.*, vol. 26, no. 5, pp. 277–279, Mar. 2001.
- [11] F. He, *et al.*, "Direct fabrication of homogeneous microfluidic channels embedded in fused silica using a femtosecond laser," *Opt. Lett.*, vol. 35, no. 3, pp. 282–284, Feb. 2010.
- [12] M. Kim, D. J. Hwang, H. Jeon, K. Hiromatsu, and C. P. Grigoropoulos, "Single cell detection using a glass-based optofluidic device fabricated by femtosecond laser pulses," *Lab Chip*, vol. 9, no. 2, pp. 311–318, 2009.
- [13] Y. Lai, K. Zhou, L. Zhang, and I. Bennion, "Microchannels in conventional single-mode fibers," *Opt. Lett.*, vol. 31, no. 17, pp. 2559–2561, Sep. 2006.
- [14] K. Zhou, Y. Lai, X. Chen, K. Sugden, L. Zhang, and I. Bennion, "A refractometer based on a micro-slot in a fiber Bragg grating formed by chemically assisted femtosecond laser processing," *Opt. Express*, vol. 15, no. 24, pp. 15848–15853, Nov. 2007.
- [15] R. Yang, Y. S. Yu, C. Chen, Q. D. Chen, and H. B. Sun, "Rapid fabrication of micro hole array structured optical fibers," *Opt. Lett.*, vol. 36, no. 19, pp. 3879–3881, Oct. 2011.